arXiv:1512.08497v1 [hep-ph] 28 Dec 2015

A Promising Interpretation of Diphoton Resonance at 750 GeV

Xiao-Jun Bi[a], Ran Ding[b], Yizhou Fan[c], Li Huang[c], Chuang Li[c], Tianjun Li[c,d], Shabbar Raza[c], Xiao-Chuan Wang[e], Bin Zhu[f]

[a] *Key Laboratory of Particle Astrophysics, Institute of High Energy Physics, Chinese Academy of Sciences, Beijing 100049, P. R. China*

[b] *Center for High-Energy Physics, Peking University, Beijing, 100871, P. R. China*

[c] *State Key Laboratory of Theoretical Physics and Kavli Institute for Theoretical Physics China (KITPC), Institute of Theoretical Physics, Chinese Academy of Sciences, Beijing 100190, P. R. China*

[d] *School of Physical Electronics, University of Electronic Science and Technology of China, Chengdu 610054, P. R. China*

[e] *Department of Physics, Henan Normal University, Xinxiang, Henan, 453007, P.R.China*

[f] *Institute of Physics, Chinese Academy of sciences, Beijing 100190, P. R. China*

Abstract

Recently, an excess of events in diphoton channel with invariant mass of about 750 GeV has been reported by the ATLAS and CMS Collaborations. Considering it as a tantalizing hint for new physics beyond the Standard Model (SM), we propose a simple extension of the SM with an additional doublet Higgs $H^{'}$ and a singlet s. We consider the neutral component $H_0^{\prime}$ of $H^{\prime}$ as the 750 GeV resonance, and assume that s is lighter than 2.6 GeV. In particular, $H_0^{\prime}$ can be produced at tree level via $q\bar{q}$ production, and decay into a pair of s at tree level. And then s can decay into a pair of collimated photons, which cannot be distinguished at the LHC. We show that the diphoton production cross section can be from 3 to 13 fb, the decay width of $H_0^{\prime}$ can be from 30 to 60 GeV, and all the current experimental constraints including dijet constraint can be satisfied.

1 Introduction

At the Run 2 of the Large Hadron Collider (LHC) with a center of mass energy of $\sqrt{s} = 13$ TeV, both the ATLAS [1] and CMS [2] Collaborations have reported an excess in diphoton channel with invariant mass of about 750 GeV. With an integrated luminosity of 3.2 fb^{-1}, the ATLAS Collaboration has observed a local 3.6σ excess at the diphoton invariant mass around 747 GeV, assuming a narrow width resonance. For a wider width resonance, the signal significance increases to 3.9σ with a preferred width about 45 GeV. Using 3.2 fb^{-1} of data, the CMS Collaboration found a diphoton excess with a local significance of 2.6σ at invariant mass around 760 GeV. Assuming the decay width around 45 GeV, the significance reduces to 2σ. The excesses in the cross sections can be roughly estimated as $\sigma^{13\ \mathrm{TeV}}_{pp\to\gamma\gamma} \sim 3 - 13$ fb [1, 2]. It is interesting to note that the CMS Collaboration did search for diphoton resonance [3] at $\sqrt{s} = 8$ TeV and observed a slight excess $\sim 2\sigma$ at an invariant mass of about 750 GeV but on the other hand the ATLAS Collaboration did not go beyond the mass of 600 GeV for this channel [4]. This indicates that the present ATLAS and CMS observations at $\sqrt{s} = 13$ TeV are consistent with their results at $\sqrt{s} = 8$ TeV for diphoton channel.

Taking these results optimistically, the excess in diphoton channels may turn out to be the rays of light showing the dawn of the new era of long awaited physics beyond the Standard Model (SM). In this study we interpret the excess of diphoton events as a hint for new physics beyond the SM. The observed resonance can be naively understood as a spin-0 or 2 particle with mass 750 GeV because of the Landau-Yang theorem [5, 6], Spurred by these interesting developments, new studies in model building for both effective and renormalizable frameworks [7, 8, 9, 10, 11, 12, 13] have been carried out. Though apparently spin-1 resonance seems to be forbidden due to Landau-Yang theorem [5, 6], it was shown in [8] that one can still trick it to obtain the diphoton excess from a vector resonance. It was pointed out in Ref. [9, 10, 11] that in scenario like 2-Higgs Doublet Model (2HDM), including the Minimal Supersymmetric Standard Model (MSSM) and the Next-to-Minimal Supersymmetric Standard Model (NMSSM), the branching ratio $Br(H/A \to \gamma\gamma)$ turns out to be very small $\mathcal{O}(10^{-6})$. It was further noted that it remains small even in the extreme case of $\tan\beta \sim 1$ which is the lower limit required by the Renormalization Group Equation (RGE) running of Yukawa couplings. In a recent paper [12], R-parity SUSY model is considered to address the diphoton excess issue.

In this paper, we propose an simple extension of the SM with an additional doublet Higgs $H^{'}$ and a singlet s. We consider the neutral component H'_0 of H' as the 750 GeV resonance, and assume that s is lighter than 2.6 GeV. Especially, H'_0 can be produced at the LHC at tree level via $q\bar{q}$ production, and decay into a pair of s at tree level. And then s can decay into a pair of collimated photons. Because s is light and highly boosted, each pair of photons may

appear as an single photon in the detector [8, 13]. We show that the diphoton production cross section can be from 3 to 13 fb, the decay width of H_0' can be from 30 to 60 GeV, and all the current experimental constraints including dijet constraint can be satisfied.

This paper is organized as follows. We devote Section 2 to describe our model. In Section 3, we investigate the diphoton signal in our model by considering constraints from the LHC at $\sqrt{s} = 8$ TeV. We also discuss the scenario where two collimated photon pairs coming from $s \to \gamma\gamma$ can be measured as two photons and can be accounted for the diphoton excess. In addition to it, we discuss two scenarios in which we can enhance $Br(s \to \gamma\gamma)$. Conclusion and summary are given in Section 4.

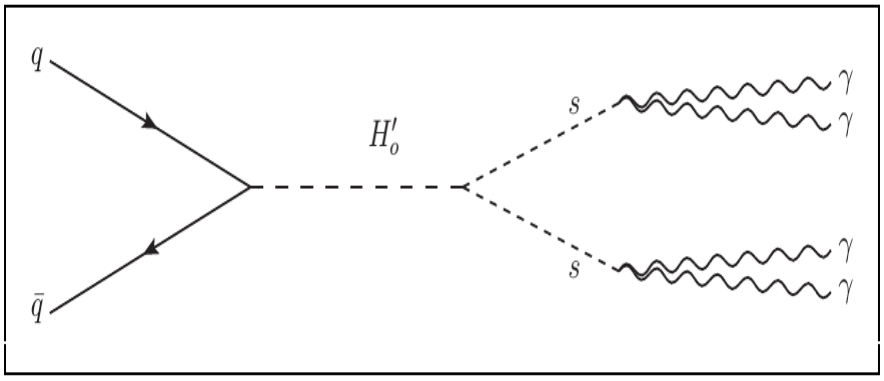

Figure 1: Feynman diagram for the process $q\bar{q} \to H_0^{'} \to ss \to \gamma\gamma\gamma\gamma$.

2 The Model Building

The model we propose here is a simple extension of the SM. This model contains two Higgs doublets, H and $H^{'}$ where H is a SM like Higgs doublet, as well as a SM real singlet s. For simplicity, we assume that $H^{'}$ will not develop a vacuum expectation value (VEV) or its VEV is negligible, and s is CP-even. The discussion for CP-odd singlet is similar. The Lagrangian of the model can be given as:

$$\begin{aligned}\mathcal{L} =&[-m_H^2|H|^2 + m_{H'}^2|H^{'}|^2 + \frac{1}{2}m_s^2 s^2 + \lambda_1|H|^4 + \lambda_2|H^{'}|^4 + \lambda_3|H|^2|\bar{H}^{'}|^2 + \lambda_4|\bar{H}^{'}H|^2] \\ &- [\frac{\lambda_5}{2}(\bar{H}^{'}H)^2 + Y_d H q\bar{d} + Y_u \bar{H} q\bar{u} + Y_e H l\bar{e} + \xi_1 \bar{H}^{'} q\bar{d} + \xi_2 H^{'} q\bar{u} + \frac{\lambda_s}{2} H^{'} H s^2 + ... + h.c]\end{aligned} \tag{1}$$

where m_H, $m_{H'}$, m_s are the masses of SM like Higgs H, the extra Higgs $H^{'}$ and the scalar s, λ_1 is the crucial quartic coupling which is fixed by the Higgs mass, $\lambda_2 - \lambda_5$ couplings are not relevant

in our present study and we set them to zero for simplicity, while $Y_{u,d}$ are the conventional Yukawa couplings. Furthermore, we also assume that $\xi = \xi_1 = \xi_2$ which are the additional couplings between the extra Higgs and quarks. Here we want to emphasize that since in our case quarks directly couple to $H^{'}$, the production rate of resonance is $(pp \to H^{'})$ is very large as compared to the conventional loop induced production, such as the gluon fusion. This is one of the distinct feature of our scenario as compared to [8]. In the last part of Eq. 1, λ_s represents the strength of the interaction of $H^{'}$, H and s. This term plays the role in determining the decay

3 A Promising Mechanism to Generate Diphoton Excess

In this section we will elaborate the mechanism we follow to address the issue of diphoton excess.

3.1 Diphoton Excess and the LHC Constraints

To estimate the diphoton signal quantitatively, we use `SARAH` [14] generate `UFO` model file [15], and `MadGraph5_aMC@NLO` [16] to calculate the production cross section of $H_0^{'}$ with `CTEQ6L1` [17] parton distribution function (PDF). We consider the diphoton cross section 3fb $< \sigma^{13}_{pp\to\gamma\gamma} <$ 13 fb and dijet constraint $\sigma^{8}_{pp\to H_0^{'}\to jj} < 5$ Pb. We display our results of calculations in $\lambda_s - \xi$ plane. Plot in the left panel is for LHC 13 TeV. In this plot red, green, blue, orange and purple colors are corresponding to ξ_u^{11}, ξ_d^{11}, ξ_u^{22}, ξ_d^{22} and $\xi_{\rm tot}$ contributions, respectively. Here, $\xi_{\rm tot}$ is the universal coupling for the first two generations. In the right panel we present the similar plot for LHC 8 TeV where the upper bound of diphoton rate is set to be 2 fb. It should be noted that for couplings of first generation quarks ξ_u^{11} and ξ_d^{11}, the viable overlapped region on the diphoton cross section and dijet constraint is smaller than that for the second generation quarks ξ_u^{22} and ξ_d^{22}. Therefore, if one combines the results of diphoton excess at 13 TeV and null result at 8 TeV, $H_0^{'}$ coupling to second generation quarks are more favored. In Fig. 3, we show the contours of total decay widths $\Gamma_{H'^0}(\xi_{u,d}^{11,22}) = 45$ GeV and $\Gamma_{H'^0}(\xi_{\rm tot}) = 45$ GeV in the $[\log_{10}\lambda_s,\ \log_{10}\xi]$ plane. For comparison, the allowed regions for the dijet constraints are also given with the same color legends in Fig. 2 for ξ_u^{22} and $\xi_{\rm tot}$, respectively. Therefore, the case with $\xi_{\rm tot}$ is entirely excluded by the dijet constraints. Interestingly, for the case with $\xi_{u,d}^{22}$, the dijet constraint can be evaded due to the PDF dependence. In short, the diphoton production cross section can be from 3 to 13 fb, the decay width of $H_0^{'}$ can be from 30 to 60 GeV, and all the current experimental constraints including dijet constraint can be satisfied.

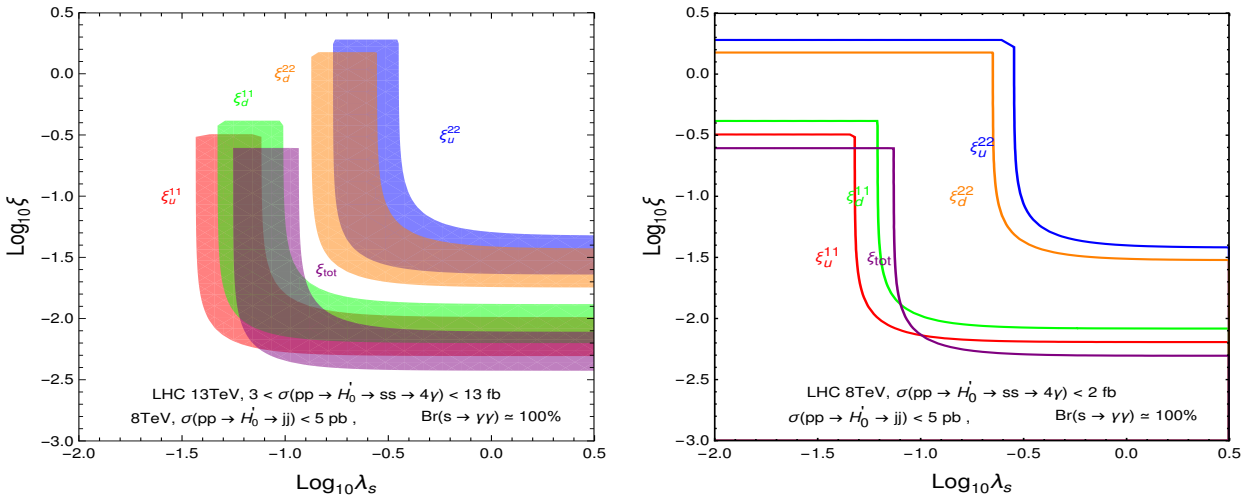
LHC 13TeV, 3 < σ(pp → H'0 → ss → 4γ) < 13 fb
8TeV, σ(pp → H'0 → jj) < 5 pb ,
Br(s → γγ) ≈ 100%
Log10ξ
Log10λs
LHC 8TeV, σ(pp → H'0 → ss → 4γ) < 2 fb
σ(pp → H'0 → jj) < 5 pb ,
Br(s → γγ) ≈ 100%
Log10ξ
Log10λs

Figure 2: Left panel: allowed region for of diphoton rate on the $[\log_{10}\lambda_s,\ \log_{10}\xi]$ plane, we take the diphoton cross section 3fb $< \sigma^{13}_{pp\to\gamma\gamma} <$ 13 fb and dijet constraint $\sigma^{8}_{pp\to H_0'\to jj} <$ 5 Pb. The red, green, blue, orange and purple colors are corresponding to ξ_u^{11}, ξ_d^{11}, ξ_u^{22}, ξ_d^{22} and $\xi_{\rm tot}$ contributions, respectively. Right panel: similar plots for the LHC 8 TeV, where the upper bound of diphoton rate is set to be 2 fb.

3.2 Collimated Photons from Boosted Scalars

In this subsection we will discuss how two pairs of photons generated from $s \to \gamma\gamma$ may be falsely detected as diphoton instead of four photons. Similar analysis is also given in Refs. [8, 13]. The main idea behind this assumption is that in decaying process, $s \to \gamma\gamma$, if the s is highly boosted, so that it travels longer before decaying and the pair of photons are highly collimated, then it is possible that the two photons when arrive at the detector may be falsely detected as a single photon. It is important to note that s can not be very long lived otherwise it will decay outside electromagnetic calorimeter (ECAL) or can not be very short lived. In that case pair of photons will not be too collimated and four gamma events will be registered instead of diphoton. Let us describe this scenario in more detail. The distribution of opening angle α between the collimated photons in the Lab frame is given as:

$$\frac{dN}{d\alpha} = \frac{\cos\frac{\alpha}{2}}{2\gamma\beta\sin^2\alpha/2\sqrt{\gamma^2\sin^2\alpha/2-1}}, \tag{2}$$

where γ and β are the boost factor and velocity of s and range of α is $[2\sin^{-1}\frac{1}{\gamma},\pi]$. For $\gamma >> 1$, $\alpha_{min} = 2\sin^{-1}\frac{1}{\gamma} \sim \frac{2}{\gamma}$. We find a difference of factor 2 in the denominator of Eq. (2) as

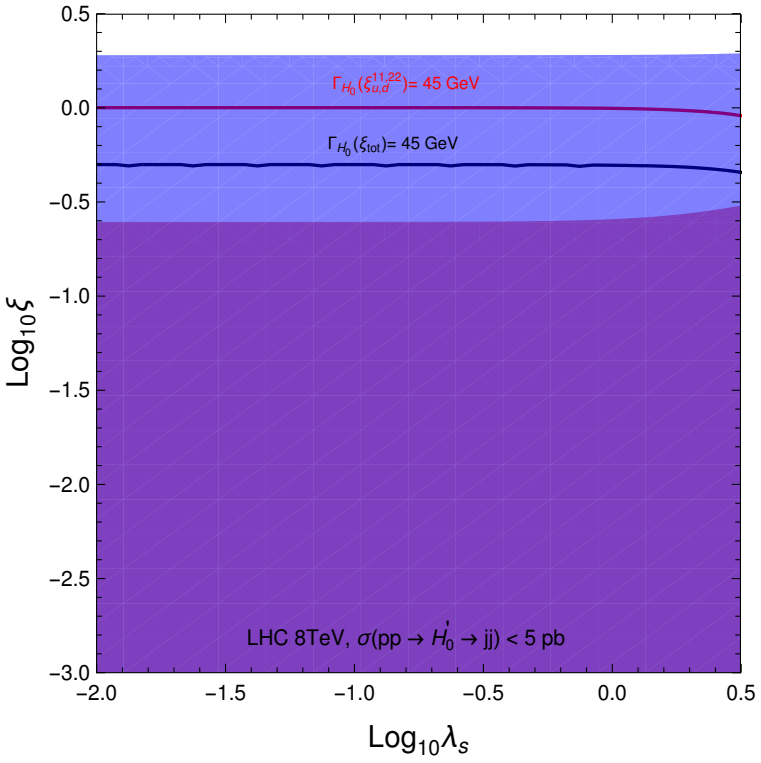

Figure 3: The contours of total decay widths $\Gamma_{H'^0}(\xi_{u,d}^{11,22}) = 45$ GeV (upper line) and $\Gamma_{H'^0}(\xi_{\rm tot}) = 45$ GeV (lower line) are presented in the $[\log_{10}\lambda_s,\ \log_{10}\xi]$ plane. For comparison, the allowed regions for the dijet constraints are also given with the same color legends in Fig. 2 for ξ_u^{22} and $\xi_{\rm tot}$, respectively.

compared to Eq. (3.1) of Ref. [8]. Integrating Eq. (2) we get:

$$N(\alpha) = \frac{\sqrt{-2+\gamma^2-\gamma^2\cos\alpha}\csc\frac{\alpha}{2}}{\sqrt{2}\beta\gamma}. \tag{3}$$

We note that for $\alpha_{mp} \approx \frac{4.6}{\gamma}$, $N(\alpha_{mp}) = 0.9$, that is for about 90% of the scalar decaying to a pair of photons, the opening angle is $\alpha \lesssim \frac{4.6}{\gamma}$. It is noted that the CMS ECAL has a resolution of $\Delta\eta \times \Delta\phi = 0.0174 \times 0.0174$ and has radius R= 1.3 meters [18] while for ATLAS has a resolution of $\Delta\eta \times \Delta\phi = 0.025 \times 0.025$ and has radius R=1.5 meters [19, 20]. If we assume the s particle flies transversely and decays to two photon. Then, the photons reach to ECAL at a distance:

$$\Delta z = \alpha_{mp}(R - \beta\gamma c\hat{\tau}) \tag{4}$$

$c\hat{\tau}$ is the proper lifetime of a particular scalar s. Note that $\beta\gamma c\hat{\tau}$ is just a decay length of s can also be given as:

$$l = \frac{\beta\gamma}{\Gamma} \tag{5}$$

where Γ is the decay width of s. Since we are assuming for simplicity that s decays perpendicular to the beam line implies $\Delta z/R < \Delta\eta$. For our case we can write Eq. (4) as

$$\begin{aligned}\Delta\eta \approx& \alpha_{mp}(1 - \frac{\beta\gamma c\hat{\tau}}{R})\\ =& \frac{4.6 m_s}{375} - \frac{4.6}{R\Gamma}\end{aligned} \tag{6}$$

Here we use the fact $\alpha_{mp} = 4.6/\gamma = 4.6 m_s/375$ and mass m_s is mass of s. From Eqs. (4) and (6), we can deduce the following two bounds

$$1 - \frac{\gamma c\hat{\tau}}{R} = 1 - \frac{375 c\hat{\tau}}{m_s R} = 1 - \frac{375}{m_s \Gamma R} > 0, \tag{7}$$

$$\Delta\eta_s \approx \frac{4.6 m_s}{375} - \frac{4.6}{\Gamma R} \leq \Delta\eta. \tag{8}$$

3.3 Enhancement of $Br(s \to \gamma\gamma)$

After discussing how two pairs of photons generated from a pair of decaying scalar may disguise themselves as diphoton, we will discuss two scenarios through which we can enhance $Br(s \to \gamma\gamma)$.

Scenario (I): In this scenario we propose to add a following term to Eq. (1)

$$\mathcal{L} = A_s s|H^{'}|^2 \tag{9}$$

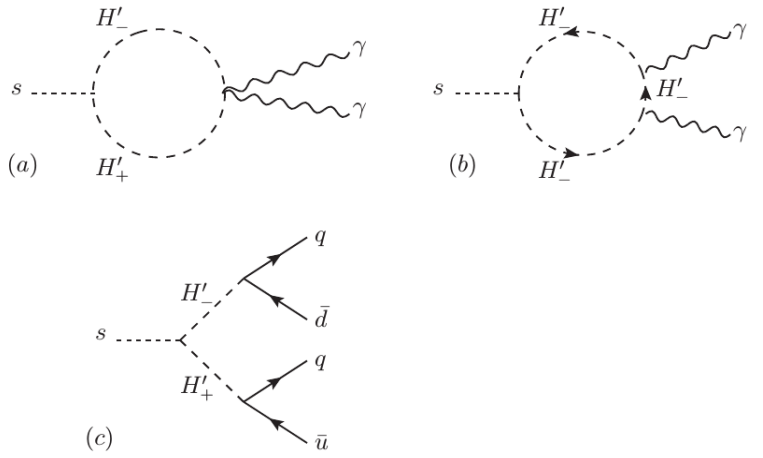

Figure 4: Feynman diagram for scenario (I).

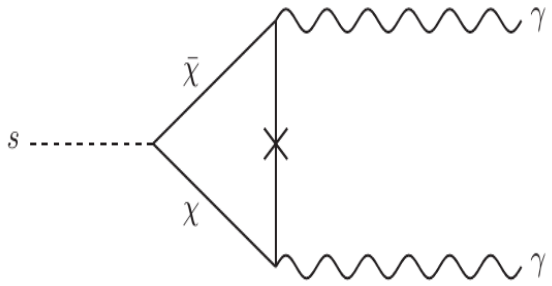

Figure 5: Feynman diagram for scenario (II).

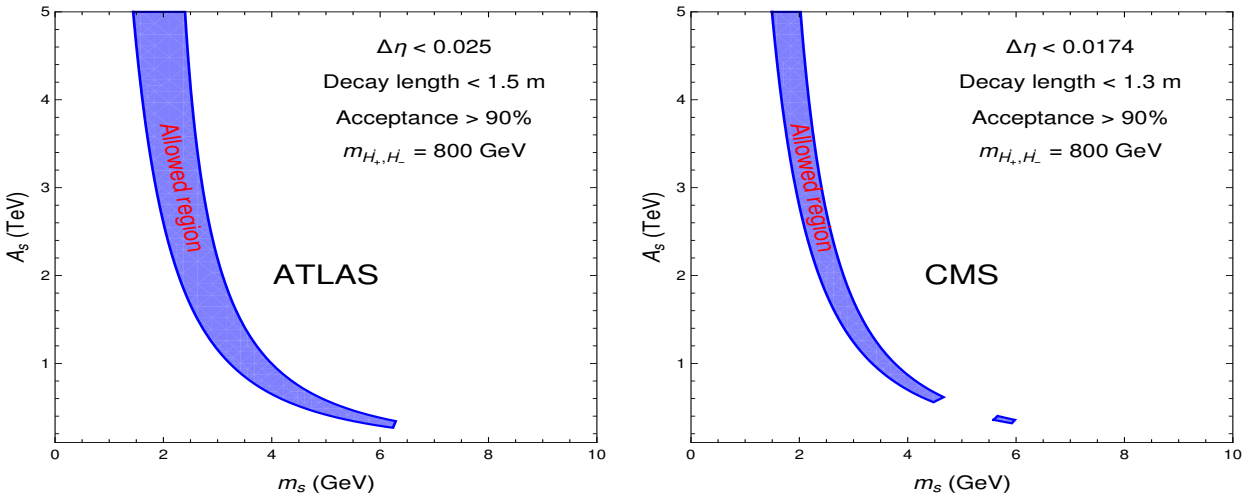

Figure 6: Plots in $m_s - A_s$ plane. Blue region represents allowed parameter space.

where A_s is a trilinear scalar coupling. The corresponding Feynman diagrams are shown in 4. In Fig. 4a,b we see that s decays to diphoton via charged Higgs loops, while Fig. 4c depicts that s can also decay to quarks respectively. Here we argue that in Fig. 4a, g_{EM} gauge coupling is involved as compared to Fig. 4b which is suppressed because of g^2_{EM}. In Fig. 4c, we see that because of off-shell charged Higgs, this diagram in general is suppressed. It should be noted that here we are considering only the second generation of quarks. Moreover, if we restrict the parameter space by imposing the kinematical constrain $m_s < 2m_c$, then the diphoton final state is the only available channel in which s can decay.

We display results of our calculations in $m_s - A_s$ plane in Fig. 6. In these plots we set $m_{H'_\pm} = 800$ GeV. In the left panel, we also use ATLAS ECAL specifications (that is radius R and $\Delta\eta$ values) related to our work as discussed in Section 3.2 and the allowed parameter space is shown in blue color. In this plot, we use Eqs. (5) and (8) to calculate decay length l of s and estimate $\Delta\eta$ and restrict ourselves to $l < 1.5$ meters and $\Delta\eta < 0.025$. Here, we see that for relatively large values of $m_s \sim 6$ GeV, the allowed $A_s \sim 400$ GeV. But as the m_s decreases, A_s starts rising up and at around $m_s \sim 2.5$ GeV, the allowed parameter space becomes essentially insensitive of A_s values. But we do note that the width of allowed band somewhat increases for small values of m_s. We present similar analysis in the right panel with the CMS ECAL specifications for R and $\Delta\eta$. Here we restrict the parameter space by imposing $l < 1.3$ meters and $\Delta\eta < 0.0174$. We immediately note that with slightly tight constraints, the allowed region of parameter space shrinks in width. It can also be seen that at about $m_s \sim 2.5$ GeV, the allowed parameter space becomes essentially insensitive of A_s values. We note that the allowed mass range for s consistent with all the current constraints discussed above is about $m_s \sim$ [1.4, 6] GeV and [1.5, 4.5] GeV for the ATLAS and CMS specifications, respectively.

Scenario (II): In this scenario we propose to add the vector-like fermions (χ, $\bar{\chi}$) with electromagnetic charges ± 1 like the right-handed charged leptons to our model by introducing the following term to Eq. (1)

$$\mathcal{L} = \lambda_\chi s \chi \bar{\chi} + m_\chi \chi \bar{\chi} \tag{10}$$

The corresponding Feynman diagram is shown in Fig. 5. Note that here we only add vector-like leptons (VLL) χ, since addition of vector-like quarks (VLQ) can generate gluon pairs and will form jets. They are highly constrained by the dijet searches. In Fig. 7, we presents our calculations in $\lambda_\chi - m_s$ plane. For these plots, we fix $m_\chi = 500$ GeV. Like Fig. 6, plot in the left panel follows the ATLAS ECAL specifications for R and $\Delta\eta$ and the plot in the right panel satisfies the CMS ECAL specifications and allowed parameter space is shown in red color band. The allowed region starts slightly widening and becomes independent of λ_χ values as m_χ moves towards smaller values. Similar behaviour can also be seen in the right panel but with

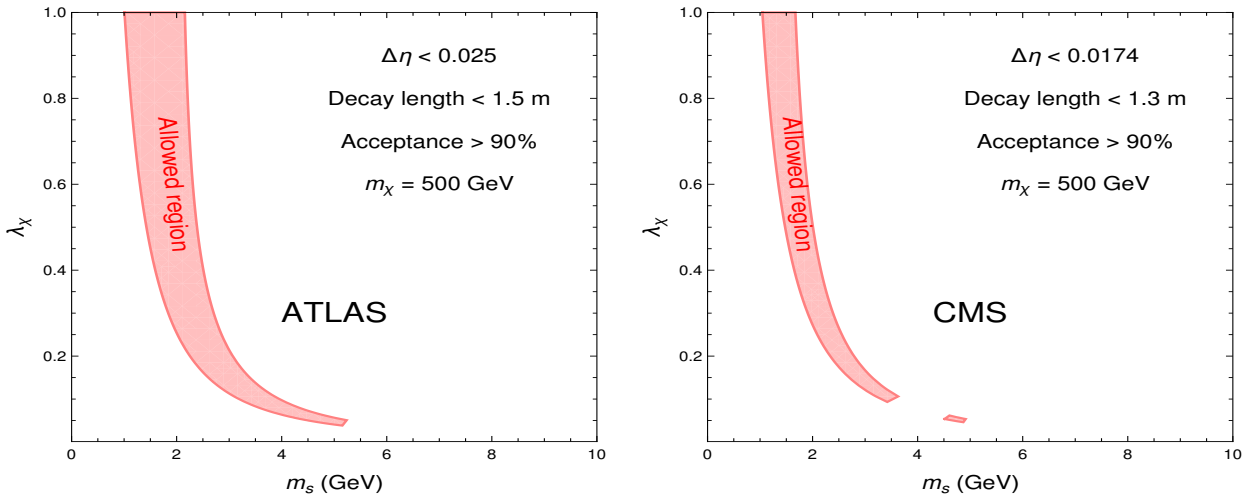

Figure 7: Plots in $m_s - \lambda_\chi$ plane. Blue region represents allowed parameter space.

somewhat narrow allowed region. We note in scenario (II), as compared to scenario (I), the maximum value of m_s is about 5 GeV for $\lambda_\chi \sim 0.05$. We see that the allowed mass range for m_s consistent with all the constrains we discussed above, $m_s \sim [1, 5]$ GeV and [1, 3.5] GeV for ATLAS and CMS specifications, respectively

4 Summary and Conclusion

An excess of events in diphoton channel with invariant mass of about 750 GeV have been reported by the ATLAS and CMS Collaborations. Considering it as a tantalizing hint for new physics beyond the SM, we proposed a SM extension with an additional doublet Higgs $H^{'}$ and a singlet s. We considered the neutral component $H_0^{\prime}$ of $H^{\prime}$ as the 750 GeV resonance, and assumed that s is lighter than 2.6 GeV. In particular, $H_0^{\prime}$ can be produced at tree level via $q\bar{q}$ production, and decay into a pair of s at tree level. And then s can decay into a pair of collimated photons. Because s is highly boosted and appropriately long lived, the pair of photons coming from a decaying scalar can be collimated enough to be measured as a single photon event in the detector. Thus, one can understand the excess in the diphoton events as a result of four photon final states instead of two photons. We showed that the diphoton production cross section can be from 3 to 13 fb, the decay width of $H_0^{\prime}$ can be from 30 to 60 GeV, and all the current experimental constraints including dijet constraint can be satisfied.

Acknowledgements– This research was supported in part by the Natural Science Foundation of China under grant numbers 11135003, 11275246, 11475238 (TL) and 11475191, 11135009 (XJB).

References

[1] ATLAS note, ATLAS-CONF-2015-081, "Search for resonances decaying to photon pairs in 3.2 fb−1 of pp collisions at $\sqrt{s} = 13$ TeV with the ATLAS detector".

[2] CMS note, CMS PAS EXO-15-004, "Search for new physics in high mass diphoton events in proton-proton collisions at 13 TeV".

[3] V. Khachatryan *et al.* [CMS Collaboration], Phys. Lett. B **750**, 494 (2015) doi:10.1016/j.physletb.2015.09.062 [arXiv:1506.02301 [hep-ex]].

[4] G. Aad *et al.* [ATLAS Collaboration], Phys. Rev. Lett. **113**, no. 17, 171801 (2014) doi:10.1103/PhysRevLett.113.171801 [arXiv:1407.6583 [hep-ex]].

[5] L. D. Landau, *On the angular momentum of a system of two photons*, *Dokl. Akad. Nauk Ser. Fiz.* **60** (1948), no. 2 207–209.

[6] C.-N. Yang, *Selection Rules for the Dematerialization of a Particle Into Two Photons*, *Phys. Rev.* **77** (1950) 242–245.

[7] L. J. Hall, K. Harigaya and Y. Nomura, arXiv:1512.07904 [hep-ph]. J. A. Casas, J. R. Espinosa and J. M. Moreno, arXiv:1512.07895 [hep-ph]. J. Zhang and S. Zhou, arXiv:1512.07889 [hep-ph]. K. Cheung, P. Ko, J. S. Lee, J. Park and P. Y. Tseng, arXiv:1512.07853 [hep-ph]. K. Das and S. K. Rai, arXiv:1512.07789 [hep-ph]. H. Davoudiasl and C. Zhang, arXiv:1512.07672 [hep-ph]. M. Cveti, J. Halverson and P. Langacker, arXiv:1512.07622 [hep-ph]. S. Chakraborty, A. Chakraborty and S. Raychaudhuri, arXiv:1512.07527 [hep-ph]. M. Badziak, arXiv:1512.07497 [hep-ph]. K. M. Patel and P. Sharma, arXiv:1512.07468 [hep-ph]. S. Moretti and K. Yagyu, arXiv:1512.07462 [hep-ph]. Q. H. Cao, S. L. Chen and P. H. Gu, arXiv:1512.07541 [hep-ph]. W. C. Huang, Y. L. S. Tsai and T. C. Yuan, arXiv:1512.07268 [hep-ph]. U. K. Dey, S. Mohanty and G. Tomar, arXiv:1512.07212 [hep-ph]. A. E. C. Hernndez and I. Nisandzic, arXiv:1512.07165 [hep-ph]. C. W. Murphy, arXiv:1512.06976 [hep-ph]. J. S. Kim, K. Rolbiecki and R. R. de Austri, arXiv:1512.06797 [hep-ph]. X. J. Bi, Q. F. Xiang, P. F. Yin and Z. H. Yu, arXiv:1512.06787 [hep-ph]. J. J. Heckman, arXiv:1512.06773 [hep-ph]. F. P. Huang, C. S. Li, Z. L. Liu and Y. Wang, arXiv:1512.06732 [hep-ph]. J. Cao, C. Han, L. Shang, W. Su, J. M. Yang and Y. Zhang, arXiv:1512.06728 [hep-ph]. F. Wang, L. Wu, J. M. Yang and M. Zhang, arXiv:1512.06715 [hep-ph]. X. F. Han and L. Wang, arXiv:1512.06587 [hep-ph]. I. Chakraborty and A. Kundu, arXiv:1512.06508 [hep-ph]. D. Barducci, A. Goudelis, S. Kulkarni and D. Sengupta, arXiv:1512.06842

[hep-ph]. W. S. Cho, D. Kim, K. Kong, S. H. Lim, K. T. Matchev, J. C. Park and M. Park, arXiv:1512.06824 [hep-ph]. W. Liao and H. q. Zheng, arXiv:1512.06741 [hep-ph]. T. F. Feng, X. Q. Li, H. B. Zhang and S. M. Zhao, arXiv:1512.06696 [hep-ph]. J. Chang, K. Cheung and C. T. Lu, arXiv:1512.06671 [hep-ph]. M. Dhuria and G. Goswami, arXiv:1512.06782 [hep-ph]. M. T. Arun and P. Saha, arXiv:1512.06335 [hep-ph]. W. Chao, arXiv:1512.06297 [hep-ph]. L. M. Carpenter, R. Colburn and J. Goodman, arXiv:1512.06107 [hep-ph]. A. Alves, A. G. Dias and K. Sinha, arXiv:1512.06091 [hep-ph]. E. Gabrielli, K. Kannike, B. Mele, M. Raidal, C. Spethmann and H. Veerme, arXiv:1512.05961 [hep-ph]. J. S. Kim, J. Reuter, K. Rolbiecki and R. R. de Austri, arXiv:1512.06083 [hep-ph]. Y. Bai, J. Berger and R. Lu, arXiv:1512.05779 [hep-ph]. D. Aloni, K. Blum, A. Dery, A. Efrati and Y. Nir, arXiv:1512.05778 [hep-ph]. A. Falkowski, O. Slone and T. Volansky, arXiv:1512.05777 [hep-ph]. J. Chakrabortty, A. Choudhury, P. Ghosh, S. Mondal and T. Srivastava, arXiv:1512.05767 [hep-ph]. L. Bian, N. Chen, D. Liu and J. Shu, arXiv:1512.05759 [hep-ph]. S. Fichet, G. von Gersdorff and C. Royon, arXiv:1512.05751 [hep-ph]. J. M. No, V. Sanz and J. Setford, arXiv:1512.05700 [hep-ph]. R. Martinez, F. Ochoa and C. F. Sierra, arXiv:1512.05617 [hep-ph]. A. Ahmed, B. M. Dillon, B. Grzadkowski, J. F. Gunion and Y. Jiang, arXiv:1512.05771 [hep-ph]. P. Cox, A. D. Medina, T. S. Ray and A. Spray, arXiv:1512.05618 [hep-ph]. A. Kobakhidze, F. Wang, L. Wu, J. M. Yang and M. Zhang, arXiv:1512.05585 [hep-ph]. S. Matsuzaki and K. Yamawaki, arXiv:1512.05564 [hep-ph]. J. Ellis, S. A. R. Ellis, J. Quevillon, V. Sanz and T. You, arXiv:1512.05327 [hep-ph]. S. Di Chiara, L. Marzola and M. Raidal, arXiv:1512.04939 [hep-ph]. R. Franceschini *et al.*, arXiv:1512.04933 [hep-ph]. K. Harigaya and Y. Nomura, arXiv:1512.04850 [hep-ph]. J. Liu, X. P. Wang and W. Xue, arXiv:1512.07885 [hep-ph]. J. Gu and Z. Liu, arXiv:1512.07624 [hep-ph]. J. de Blas, J. Santiago and R. Vega-Morales, arXiv:1512.07229 [hep-ph]. P. S. B. Dev and D. Teresi, arXiv:1512.07243 [hep-ph]. S. M. Boucenna, S. Morisi and A. Vicente, arXiv:1512.06878 [hep-ph]. M. Bauer and M. Neubert, arXiv:1512.06828 [hep-ph]. J. M. Cline and Z. Liu, arXiv:1512.06827 [hep-ph]. L. Berthier, J. M. Cline, W. Shepherd and M. Trott, arXiv:1512.06799 [hep-ph]. J. S. Kim, K. Rolbiecki and R. R. de Austri, arXiv:1512.06797 [hep-ph]. O. Antipin, M. Mojaza and F. Sannino, arXiv:1512.06708 [hep-ph]. D. Bardhan, D. Bhatia, A. Chakraborty, U. Maitra, S. Raychaudhuri and T. Samui, arXiv:1512.06674 [hep-ph]. H. Han, S. Wang and S. Zheng, arXiv:1512.06562 [hep-ph]. S. Chang, arXiv:1512.06426 [hep-ph]. C. Han, H. M. Lee, M. Park and V. Sanz, arXiv:1512.06376 [hep-ph]. J. Bernon and C. Smith, arXiv:1512.06113 [hep-ph]. E. Megias, O. Pujolas and M. Quiros, arXiv:1512.06106 [hep-

ph]. R. Benbrik, C. H. Chen and T. Nomura, arXiv:1512.06028 [hep-ph]. C. Csaki, J. Hubisz and J. Terning, arXiv:1512.05776 [hep-ph]. D. Curtin and C. B. Verhaaren, arXiv:1512.05753 [hep-ph]. W. Chao, R. Huo and J. H. Yu, arXiv:1512.05738 [hep-ph]. S. V. Demidov and D. S. Gorbunov, arXiv:1512.05723 [hep-ph]. Q. H. Cao, Y. Liu, K. P. Xie, B. Yan and D. M. Zhang, arXiv:1512.05542 [hep-ph]. CMS Collaboration [CMS Collaboration], collisions at 13TeV," CMS-PAS-EXO-15-004. B. Dutta, Y. Gao, T. Ghosh, I. Gogoladze and T. Li, arXiv:1512.05439 [hep-ph]. S. D. McDermott, P. Meade and H. Ramani, arXiv:1512.05326 [hep-ph]. T. Higaki, K. S. Jeong, N. Kitajima and F. Takahashi, arXiv:1512.05295 [hep-ph]. E. Molinaro, F. Sannino and N. Vignaroli, arXiv:1512.05334 [hep-ph]. A. Belyaev, G. Cacciapaglia, H. Cai, T. Flacke, A. Parolini and H. Serdio, arXiv:1512.07242 [hep-ph]. B. C. Allanach, P. S. B. Dev, S. A. Renner and K. Sakurai, arXiv:1512.07645 [hep-ph]. M. x. Luo, K. Wang, T. Xu, L. Zhang and G. Zhu, arXiv:1512.06670 [hep-ph]. G. M. Pelaggi, A. Strumia and E. Vigiani, arXiv:1512.07225 [hep-ph]. B. Bellazzini, R. Franceschini, F. Sala and J. Serra, arXiv:1512.05330 [hep-ph]. A. Pilaftsis, arXiv:1512.04931 [hep-ph]. M. Backovic, A. Mariotti and D. Redigolo, arXiv:1512.04917 [hep-ph]. K. Harigaya and Y. Nomura, arXiv:1512.04850 [hep-ph]. Y. Mambrini, G. Arcadi and A. Djouadi, arXiv:1512.04913 [hep-ph].

[8] M. Chala, M. Duerr, F. Kahlhoefer and K. Schmidt-Hoberg, arXiv:1512.06833 [hep-ph].

[9] A. Angelescu, A. Djouadi and G. Moreau, arXiv:1512.04921 [hep-ph].

[10] R. S. Gupta, S. Jger, Y. Kats, G. Perez and E. Stamou, arXiv:1512.05332 [hep-ph].

[11] W. Altmannshofer, J. Galloway, S. Gori, A. L. Kagan, A. Martin and J. Zupan, arXiv:1512.07616 [hep-ph].

[12] R. Ding, L. Huang, T. Li and B. Zhu, arXiv:1512.06560 [hep-ph].

[13] P. Agrawal, J. Fan, B. Heidenreich, M. Reece and M. Strassler, arXiv:1512.05775 [hep-ph].

[14] F. Staub, Comput. Phys. Commun. **184**, 1792 (2013) doi:10.1016/j.cpc.2013.02.019 [arXiv:1207.0906 [hep-ph]]. F. Staub, Comput. Phys. Commun. **185**, 1773 (2014) doi:10.1016/j.cpc.2014.02.018 [arXiv:1309.7223 [hep-ph]].

[15] C. Degrande, C. Duhr, B. Fuks, D. Grellscheid, O. Mattelaer and T. Reiter, Comput. Phys. Commun. **183**, 1201 (2012) [arXiv:1108.2040 [hep-ph]].

[16] J. Alwall, M. Herquet, F. Maltoni, O. Mattelaer and T. Stelzer, JHEP **1106**, 128 (2011) [arXiv:1106.0522 [hep-ph]]; J. Alwall, R. Frederix, S. Frixione, V. Hirschi, F. Maltoni,

O. Mattelaer, H.-S. Shao and T. Stelzer *et al.*, JHEP **1407**, 079 (2014) [arXiv:1405.0301 [hep-ph]].

[17] P. M. Nadolsky, H. L. Lai, Q. H. Cao, J. Huston, J. Pumplin, D. Stump, W. K. Tung and C.-P. Yuan, Phys. Rev. D **78**, 013004 (2008) doi:10.1103/PhysRevD.78.013004 [arXiv:0802.0007 [hep-ph]].

[18] V. Khachatryan *et al.* [CMS Collaboration], JINST **10**, no. 08, P08010 (2015) doi:10.1088/1748-0221/10/08/P08010 [arXiv:1502.02702 [physics.ins-det]].

[19] G. Aad *et al.* [ATLAS Collaboration], arXiv:0901.0512 [hep-ex].

[20] G. Aad *et al.* [ATLAS Collaboration], Phys. Rev. D **83**, 052005 (2011) doi:10.1103/PhysRevD.83.052005 [arXiv:1012.4389 [hep-ex]].